

University of Nebraska - Lincoln

DigitalCommons@University of Nebraska - Lincoln

ANDRILL Research and Publications

Antarctic Drilling Program

2011

Sequence stratigraphy of the ANDRILL AND-2A drillcore, Antarctica: A long-term, ice-proximal record of Early to Mid-Miocene climate, sea-level and glacial dynamism

Christopher R. Fielding

University of Nebraska-Lincoln, cfielding2@unl.edu

Greg H. Browne

GNS Science

Brad Field

GNS Science

F. Florindo

Istituto Nazionale di Geofisica e Vulcanologia, florindo@ingv.it

D. M. Harwood

University of Nebraska at Lincoln, dharwood1@unl.edu

See next page for additional authors

Follow this and additional works at: <https://digitalcommons.unl.edu/andrillrespub>

 Part of the Environmental Indicators and Impact Assessment Commons

Fielding, Christopher R.; Browne, Greg H.; Field, Brad; Florindo, F.; Harwood, D. M.; Krissek, L. A.; Levy, Richard; Panter, K.; Passchier, Sandra; and Pekar, Stephen F., "Sequence stratigraphy of the ANDRILL AND-2A drillcore, Antarctica: A long-term, ice-proximal record of Early to Mid-Miocene climate, sea-level and glacial dynamism" (2011). *ANDRILL Research and Publications*. 43.
<https://digitalcommons.unl.edu/andrillrespub/43>

This Article is brought to you for free and open access by the Antarctic Drilling Program at DigitalCommons@University of Nebraska - Lincoln. It has been accepted for inclusion in ANDRILL Research and Publications by an authorized administrator of DigitalCommons@University of Nebraska - Lincoln.

Authors

Christopher R. Fielding, Greg H. Browne, Brad Field, F. Florindo, D. M. Harwood, L. A. Krissek, Richard Levy, K. Panter, Sandra Passchier, and Stephen F. Pekar

Submitted August 12, 2010; revised March 18, 2011; accepted March 20, 2011; published online March 24, 2011.

Sequence stratigraphy of the ANDRILL AND-2A drillcore, Antarctica: A long-term, ice-proximal record of Early to Mid-Miocene climate, sea-level and glacial dynamism

Christopher R. Fielding,¹ Greg H. Browne,² Brad Field,² Fabio Florindo,³ David M. Harwood,¹
Lawrence A. Krissek,⁴ Richard H. Levy,² Kurt S. Panter,⁵ Sandra Passchier,⁶ and Stephen F. Pekar⁷

1. Department of Earth & Atmospheric Sciences, 214 Bessey Hall, University of Nebraska-Lincoln, NE 68588-0340, USA

2. GNS Science, P.O. Box 30368, Lower Hutt, New Zealand

3. Instituto Nazionale di Geofisica e Vulcanologia, Via di Vigna Murata 605, I-00143 Rome, Italy

4. School of Earth Sciences, Ohio State University, 125 South Oval Mall, Columbus, OH 43210, USA

5. Department of Geology, Bowling Green State University, Bowling Green, OH 43403, USA

6. Department of Earth & Environmental Sciences, Montclair State University, 252 Mallory Hall, 1 Normal Avenue, Montclair, NJ 07043, USA

7. School of Earth & Environmental Sciences, Queen's College, 65-30 Kissena Blvd., Flushing, NY 11367, USA

Corresponding author — C. Fielding, cfielding2@unl.edu

Abstract

Present understanding of Antarctic climate change during the Early to Mid-Miocene, including major cycles of glacial expansion and contraction, relies in large part on stable isotope proxies from deep sea core drilling. Here, we summarize the lithostratigraphy of the ANDRILL Southern McMurdo Sound Project drillcore AND-2A. This core offers a hitherto unavailable ice-proximal stratigraphic archive from a high-accommodation continental margin setting, and provides clear evidence of repeated fluctuations in climate, ice expansion/contraction and attendant sea-level change over the period c. 20.2–14.2 Ma, with a more fragmentary record of Late Miocene and Pliocene time. The core is divided into seventy-four high-frequency (fourth- or fifth-order) glacimarine sequences recording repeated advances and retreats of glaciers into and out of the Victoria Land Basin. The section can be resolved into thirteen longer-term, composite (third-order) sequences, which comprise packages of higher frequency sequences that show a consistent stratigraphic stacking pattern (Stratigraphic Motif). The distribution of the six recognized motifs indicates intervals of less and more ice-proximal, and temperate to subpolar/polar climate, through the Miocene period. The core demonstrates a dynamic climate regime throughout the Early to Mid-Miocene that may be correlated to some previously-recognized events such as the Mid-Miocene Climatic Optimum, and provides a detailed reference point from which to evaluate stable isotope proxy records from the deep-sea.

Keywords: Miocene, Antarctica, Sequence stratigraphy, Cyclicity, Mid-Miocene Climatic Optimum, ANDRILL SMS project

1. Introduction

The Miocene glacial history of Antarctica is incompletely known and interpretations of environmental change, including expansions and contractions in glacial ice volume, rely to a considerable extent on proxy geochemical records from deep ocean ODP cores (e.g., Miller et al., 1991; Abreu and Anderson, 1998; Zachos et al., 2001; Lear et al., 2004), among others). Although stable isotope excursions have been noted within the Early Miocene record (e.g., Miller et al., 1991, 1996), there has been little opportunity to evaluate the near-field (Antarctic margin) record of these events. A warm climatic optimum is thought to have characterized the Mid-Miocene (Mid-Miocene Climatic Optimum – MMCO (~17.0–14.5 Ma)), and is also reflected by the “Monterey carbon isotope excursion” (Vincent and Berger, 1985; Woodruff and Savin, 1991; Holbourn et al., 2007). This period entailed a complex climatic optimum succeeded by a long-term climatic deterioration towards colder icehouse conditions

(Flower and Kennett, 1994; Shevenell et al., 2004; Holbourn et al., 2007). The MMCO comprises a series of maxima and minima in $\delta^{18}\text{O}$ records, suggesting a complex history of ice sheet fluctuation, but no near-field, high-resolution, Antarctic stratigraphic record of this time interval has yet been documented.

The Mid-Miocene climatic transition (14.5–13.0 Ma) is regarded by some as the time of permanent establishment of the cold polar regime of today in the East Antarctic Ice Sheet (Sugden et al., 1993; Lewis et al., 2008). Others, however, believe that warmer conditions returned in the Late Miocene through Early Pliocene, with the onset of the current “deep-freeze” regime only in the Late Pliocene (Webb et al., 1984; and see review by Barrett, 1996). Recovery of an expanded Miocene and younger stratigraphic archive from the Antarctic continental margin is therefore a high priority for current research efforts.

Much recent effort has been devoted to recovering core archives of Cenozoic paleoenvironmental change from the McMurdo Sound region of Antarctica. This area has been an attrac-

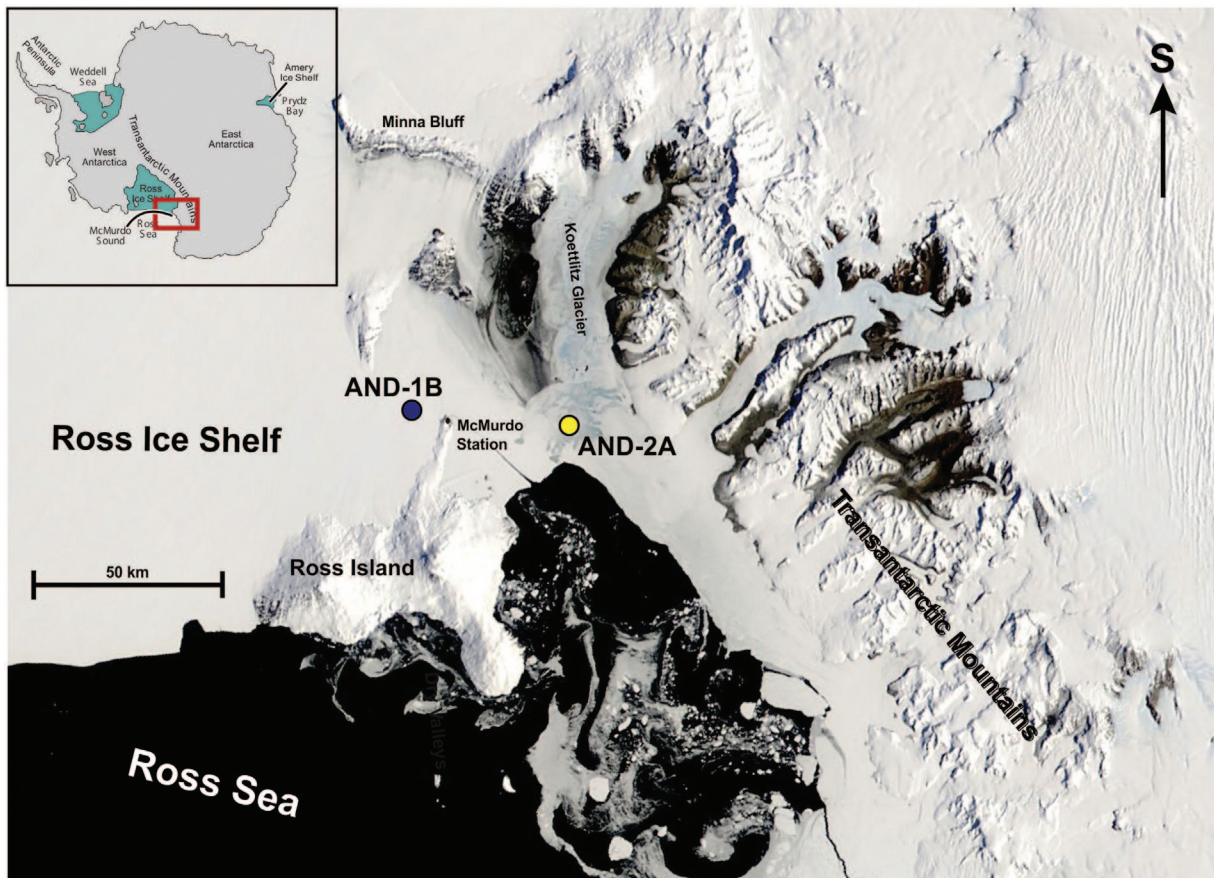


Figure 1. Aerial image showing the location of the SMS drillsite in the context of McMurdo Sound and the Ross Sea (inset map). AND-2A and the earlier AND-1B are located in the westernmost compartment of the West Antarctic Rift, termed the Victoria Land Basin, which abuts the Transantarctic Mountains. Base is a NASA MODIS image, acquired in January 2008.

tive target for core drilling because it overlies a rift basin with a > 3 km thick Cenozoic succession and because it is adjacent to the major Antarctic research bases of the USA (McMurdo Station) and New Zealand (Scott Base). The Victoria Land Basin (VLB) is one of three major sub-basins of the West Antarctic Rift system, a failed Cenozoic rift (Cooper et al., 1987). Initially land-based, shallow coring programs in the region (Dry Valleys Drilling Program, Eastern Taylor Valley Program) were succeeded by more ambitious and technologically advanced drilling operations based on fast sea-ice platforms (CIROS-1 and -2, MSSTS-1, and Cape Roberts Project -1, -2/2A and -3; Barrett, 1986, 1989, 2009; Barrett and Hambrey, 1992). The latest generation of drilling programs has taken place in the past 5 years under the auspices of the ANDRILL Program: <http://www.andrill.org>. Also, integration of drilling records with an extensive array of seismic reflection data has allowed division of the VLB stratigraphy into a series of age-constrained tectono-stratigraphic units reflecting discrete phases of basin-forming activity. The principal phases are 1) Early Rift (34–29 Ma), 2) Main Rift (29–24 Ma), 3) Passive Thermal Subsidence (24–13 Ma), and 4) Renewed Rifting (Terror Rift: 13 Ma to present) (Fielding et al., 2006, 2008a; Henrys et al., 2007).

The ANDRILL Program drilled its second hole (AND-2A) in October–November, 2007, during the coring phase of the Southern McMurdo Sound Project (SMS: Figure 1). Drilling was conducted from a fast sea-ice platform, using a custom-built drilling system that permitted the recovery of a sediment and rock core to 1138.54 meters below sea floor (mbfs) with 98% recovery (Harwood et al., 2008). Geochronological data, specifi-

cally a suite of Ar–Ar isotope ages, Sr isotope stratigraphy, biostratigraphic data from diatoms and foraminifera, and magnetostratigraphy, indicate that the core extends back to ~20 Ma, with an expanded record of the interval 20–14.2 Ma and a more fragmentary record of the interval 14.2–0 Ma (Acton et al., 2008; Di Vincenzo et al., 2010; SMS Science Team, 2010, Figure 2). The AND-2A core therefore fills a gap in understanding between the latest Eocene to Early Miocene (34–17 Ma) captured by the Cape Roberts Project in the 1990's (Barrett, 2007) and the younger section (14–0 Ma) intersected by the first ANDRILL hole (AND-1B) recovered during the McMurdo Ice Shelf Project (MIS: Figure 1; Naish et al., 2007).

A facies analysis and preliminary stratigraphic analysis of the AND-2A core is documented in Harwood et al. (2008), and a more detailed treatment of lithofacies and interpreted environments of deposition, proximity of glacial ice to the drill-site, and glacial thermal regime is given by Passchier et al. (in press). In the present paper, we build on this framework and describe a sequence stratigraphic analysis of the core drawing on existing stratigraphic models derived from the VLB succession. We interpret stratigraphic patterns in terms of long-term variability in climate, ice margin oscillations, and relative sea-level. We show changes in the stratal stacking patterns within and among genetic sequences through time, and relate these to climatic events including some inferred previously from studies of deep sea cores. A major outcome of this work is a record of dynamic climate fluctuation throughout the time interval 20–14.5 Ma, including a record of periods considerably warmer than present.

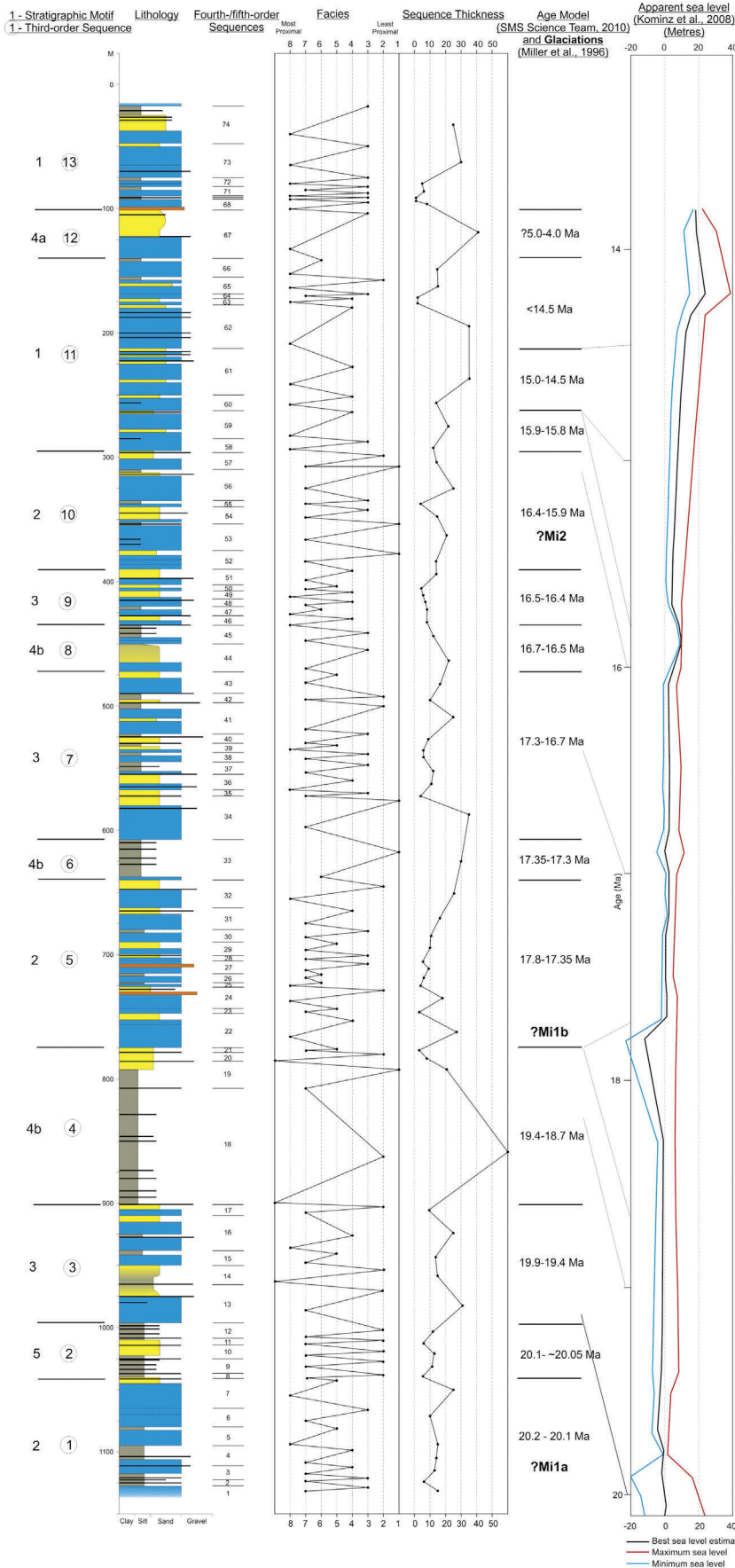


Figure 2. Summary graphic log of the AND-2A (SMS) core, showing the initial age model, division of the succession into high-frequency (fourth- to fifth-order) sequences, the inferred most ice-proximal and least ice-proximal facies in each sequence, sequence thickness, the global eustatic sea-level curve of Kominz et al. (2008). The AND-2A core is divided into a succession of thirteen composite (third-order) sequences (reflecting major changes in these and other parameters (see Table 3 and text for discussion)). Age ranges are modified after SMS Science Team (2010). Lithology codes: Olive gray – mudrock, yellow – sandstone, blue – diamictite, orange – conglomerate/breccia. Depth in meters below sea floor.

1.1. Lithologies and sequence definition

The AND-2A core preserves a variety of terrigenous clastic lithologies, ranging from claystone, through siltstone and sandstone to conglomerate, breccia and diamictite (Figure 2). Absolute ages have been obtained from first-cycle volcanic components by the Ar-Ar method (Di Vincenzo et al., 2010). Thirteen recurring facies have been recognized and interpreted in terms of depositional environments ranging from minimally ice-influenced, shallow marine settings, through ice-contact proglacial and glacimarine, to possibly subglacial environments (Table 1). Some mudrocks in particular (Facies 1; Table 1) lack dispersed gravel, are richly fossiliferous (marine mollusks, polychaetes, foraminifera and marine diatoms) and extensively and diversely bioturbated, suggesting times of minimal ice influence. Some diamictites show extensive boxwork veining, brecciation, shear and rotation fabrics suggesting that the drillsite was covered by grounded ice at times (Facies 7/8; Table 1). The entire section, including the near-surface, shows evidence of deposition in shelf water depths (10–100 m; Table 1; Taviani et al., 2008; Fielding et al., 2008b). Detailed descriptions and process/environmental interpretations of these facies are given by Passchier et al. (in press).

A repetitive vertical stacking pattern of lithofacies (Table 1; Figure 3; Figure 4) in the SMS core was observed, allowing the division of the succession into sequences (in the Vail-EXXON sense; cf. Catuneanu et al., 2009). In the idealized form of a complete sequence (Figure 5), the base of each sequence (the sequence boundary) is defined at a point where there is an abrupt upward transition from finer- to coarser-grained lithology. Lithologies immediately overlying the sequence boundary are commonly the coarsest-grained in the sequence. Typically, the sequence boundary lies at the base of a diamictite unit but in a few cases the base is recorded by another coarse-grained lithology. The upper portion of the diamictite body in places is interbedded with conglomerate and sandstone and fines upward through sandstones into mudrocks, typically with dispersed gravel. Overlying these facies are the finest-grained fa-

cies in the sequence, typically, fine-grained siltstones that are lacking in any gravel, are bioturbated and often contain marine invertebrate shells. Mudrocks coarsen upward into a sandstone-dominated interval showing extensive preservation of current and wave-generated sedimentary structures, and this section is then abruptly (in many cases, erosional/irregularly) truncated by the next sequence boundary. Overall, thicker and more complete cycles (sequences) were noted from the lower part of the core, becoming thinner and less complete upward (with some notable exceptions). An idealized form of the complete sequence is presented as Figure 5.

The interpretation of sequences in this near-ice, glacimarine context is based on a sequence stratigraphic model first proposed by Fielding et al., (1998, 2000) and modified by Dunbar et al. (2008) for the Cape Roberts Project cores further north and also on the VLB margin (Figure 1). In this model, repetitive stratal stacking patterns are interpreted in terms of advances and retreats of glaciers into and out of the basin, with attendant relative sea-level changes. Dunbar et al. (2008) used mud content of core samples as a proxy for wave-induced bed shear stress which, for a given wave climate, is proportional to water depth (Dunbar and Barrett, 2005), and inferred ranges of paleobathymetric variation of the order of tens of meters within sequences defined on the basis of facies changes. The premise that underpins this model is that the facies indicating ice-minimal conditions invariably are also those indicating deepest water environments of formation, and vice-versa, suggesting eustatic sea-level fluctuation exerted a fundamental control on the glacimarine stratigraphic record of the VLB. This approach has been found to be useful for characterizing the repetitive stratigraphic sections recovered from more recent VLB cores (e.g., Naish et al., 2008, 2009; McKay et al., 2009). The general observation that Cenozoic stratigraphic successions in the VLB show clear cyclicity with predictable vertical arrangements of facies, becoming less so inboard towards the present coastline and onshore (e.g., McGinnis, 1981; Fielding et al., in press), suggests that a coherent record of sea-level fluctuation is preserved in the high-accommodation setting of the VLB.

Table 1. List of lithofacies recognized in the AND-2A core. Estimates of formative water depths are based on analogy with calculations of Dunbar et al. (2008).

Facies	Description	Interpretation
1	Diatomite, opal-bearing or calcareous, fossil-rich mudstone, typically intensively and diversely bioturbated, little if any dispersed gravel	Open marine shelfal conditions (60–100 m water depth), minimal ice influence
2	Siltstone to very fine-grained sandstone, intensively and diversely bioturbated, dispersed small gravel and calcareous fossils, soft-sediment deformation structures	Open marine shelfal conditions (60–100 m water depth), deposition from suspension settling, distal ice influence
3	Interstratified siltstone and very fine- to fine-grained sandstone, bioturbated and/or stratified with ripple-scale structures, typically restricted and modest intensity bioturbation, dispersed calcareous fossils, soft-sediment deformation	Open marine to restricted coastal settings (10–80 m water depth), deposition from suspension settling, and gentle currents and waves, minor ice rafting
4	Stratified, fine- to coarse-grained sandstone, dispersed to locally concentrated small gravel, typically well sorted, with flat lamination, ripple cross-lamination, cross-bedding and hummocky cross-stratification, minimal bioturbation, locally fossiliferous	Open marine shoreface to upper offshore (10–40 m water depth), minor ice rafting of gravel
5	Muddy fine-grained sandstone to sandy siltstone with dispersed gravel, typically soft-sediment-deformed or unstratified, locally fossiliferous, rarely bioturbated	Open marine conditions (10–60 m water depth) affected by hemipelagic fallout and supply of sediment from ice-rafting
6	Delicately stratified, interlaminated fine- and coarse-grained siltstone, fine-grained sandstone and diamictite, dispersed gravel including diamictite clasts, some lamination rhythmic at sub-mm scale, soft-sediment and brittle deformation	Open glacimarine conditions affected by hemipelagic fallout, bottom currents and ice-rafting
7	Stratified diamictite, generally clast-poor, muddy to sandy matrix, commonly fossiliferous	Open, proximal glacimarine conditions, in distal portions of grounding-line fans
8	Massive diamictite, clast-poor to clast-rich and typically sandy matrix, some alignment of clast long-axes, shear structures including boxwork fracturing and brecciation	Ice-proximal glacimarine (grounding-line fan) to subglacial environments
9	Interbedded conglomerate and sandstone, thin units typically interbedded with other coarse-grained facies, locally fossiliferous	Ice-proximal environments in the presence of meltwater, various possible depositional settings
10	Vesicular, porphyritic, and basaltic lava	Primary sheet flows erupted from a proximal vent or fissure
11	Volcaniclastic breccias, monomict, composed of basaltic clasts in basaltic matrix	Autobrecciation of subaerially erupted lavas
12	Pyroclastic lapilli tuff, composed of glassy juvenile clasts of coarse ash to lapilli size	Settling of pyroclasts through the water column
13	Volcanic sedimentary breccias and sandstones, comprising texturally unmodified to modified juvenile volcanic clasts and grains, local ripple cross-lamination	Reworking of volcaniclastic deposits in shallow marine waters

Relative sea level changes in glaciated regions can be expected to record a convolution of eustatic effects created by withdrawal of sea-water to form ice during glacial intervals and subsequent melting during deglacial periods, along with isostatic, self-gravitational, and solid-earth deformational effects (e.g., Mitrovica and Vermeersen, 2002; Bamber et al., 2009; Mitrovica et al., 2009). The magnitude, and spatial and temporal range of isostatic and gravitational effects are expected to vary according to the lateral extent of glacial ice (for example, whether or not it extended into the basin), and its thickness distribution (Brotchie and Silvester, 1969; Andrews, 1974). It is also likely that isostatic effects may have varied according to the thermal properties of the underlying lithosphere, and hence according to tectonic context. The study area is likely to have been characterized by a thinned and heated lithosphere during the formation of the extensional VLB, which may have dampened isostatic effects. Other processes mentioned above are also likely to have played a role in determining relative sea-level changes during glacial-nonglacial or glacial-interglacial cycles, but the net effect of these processes in combination cannot be calculated from available knowledge.

Each sequence boundary is interpreted to record a relative sea-level minimum. It is further interpreted to be a composite, time-transgressive surface in the manner now known to be typical of sequence boundaries in general, recording a perhaps protracted relative sea-level drawdown and lowstand (Catuneanu et al., 2009). Since the sequence boundary is typically overlain by a diamictite, the sequence boundary must also record a glacial advance into the basin. Given the known capacity of grounded glaciers to erode substantial quantities of previously-deposited sediment and transport them in a basinward direction as they advance (Lønne and Syvitski, 1997; Lønne, 2001), it is to be expected that the surface recording such an advance will be an erosional contact in locations where ice has overridden the site. For this reason, Fielding et al. (2000) coined the term "Glacial Surface of Erosion" (GSE) for such surfaces (and see Naish et al., 2009). In more ice-distal locations, beyond the maximum extent of glacier advance, the contact need not be erosional, however, but rather is a sharp, planar contact or even a gradational coarsening-upward contact between ice-distal and more ice-proximal facies. For this reason, we elect not to adopt the GSE terminology herein.

The position of the glacial maximum in any given sequence may not be easy to determine, depending upon whether there is any preserved evidence of subglacial deposition recording ice grounding at the site of investigation, and taking into account that the maximum ice advance may not have a stratigraphic record. In an ice-proximal depositional setting, furthermore, a number of additional influences on relative sea-level change come into play as discussed above, the net effect of which cannot be ascertained.

In VLB Cenozoic sequences, stratal stacking patterns above the basal diamictite or equivalent are typically fining-upward then coarsening-upward (interpreted as recording deepening followed by shallowing), consistent with the relative sea-level fluctuations expected from a postglacial sea-level rise superimposed on a regime of steady subsidence. This in turn suggests that gravitational and isostatic effects (both loading and unloading, the magnitude of which should be similar) could be entirely contained within the hiatal surface of the sequence boundary and in the overlying diamictite. Accordingly, the basal diamictite is interpreted as a combination of Lowstand Systems Tract (LST) and early Transgressive Systems Tract (TST) deposits (Figure 5). This assumption is likely an oversimplification. Nonetheless, it is consistent with stratal stacking patterns and in the absence of a more refined model of the behavior of the Antarctic continental margin under repeated loading and unloading by glacial ice, is adopted here. An alternative model, in which the fining-upward interval is the product of flexural loading during the glacial maximum and the overlying coarsening-upward interval a consequence of subsequent, postglacial isostatic rebound, is rejected because such an interpretation is inconsistent with the distribution of glacial sedimentological indicators including the abundance of

limestone. The overlying, fining-upward interval records progressively increasing paleo-water depth, with an increasing component of hemipelagic fallout (of terrigenous clastic, biochemical, and at times volcanioclastic origin), and is less influenced by lateral transport of sediment along the seabed. This interval is also assigned to the TST. Above this, an interval of finest-grained sediment with little if any evidence of ice rafting is interpreted to represent the maximum flooding zone (MFZ) following an ice retreat or deglaciation event. The expression "Maximum Flooding Zone" is used here rather than "Maximum Flooding Surface" because it is typically not possible to recognize a single surface that records maximum marine transgression.

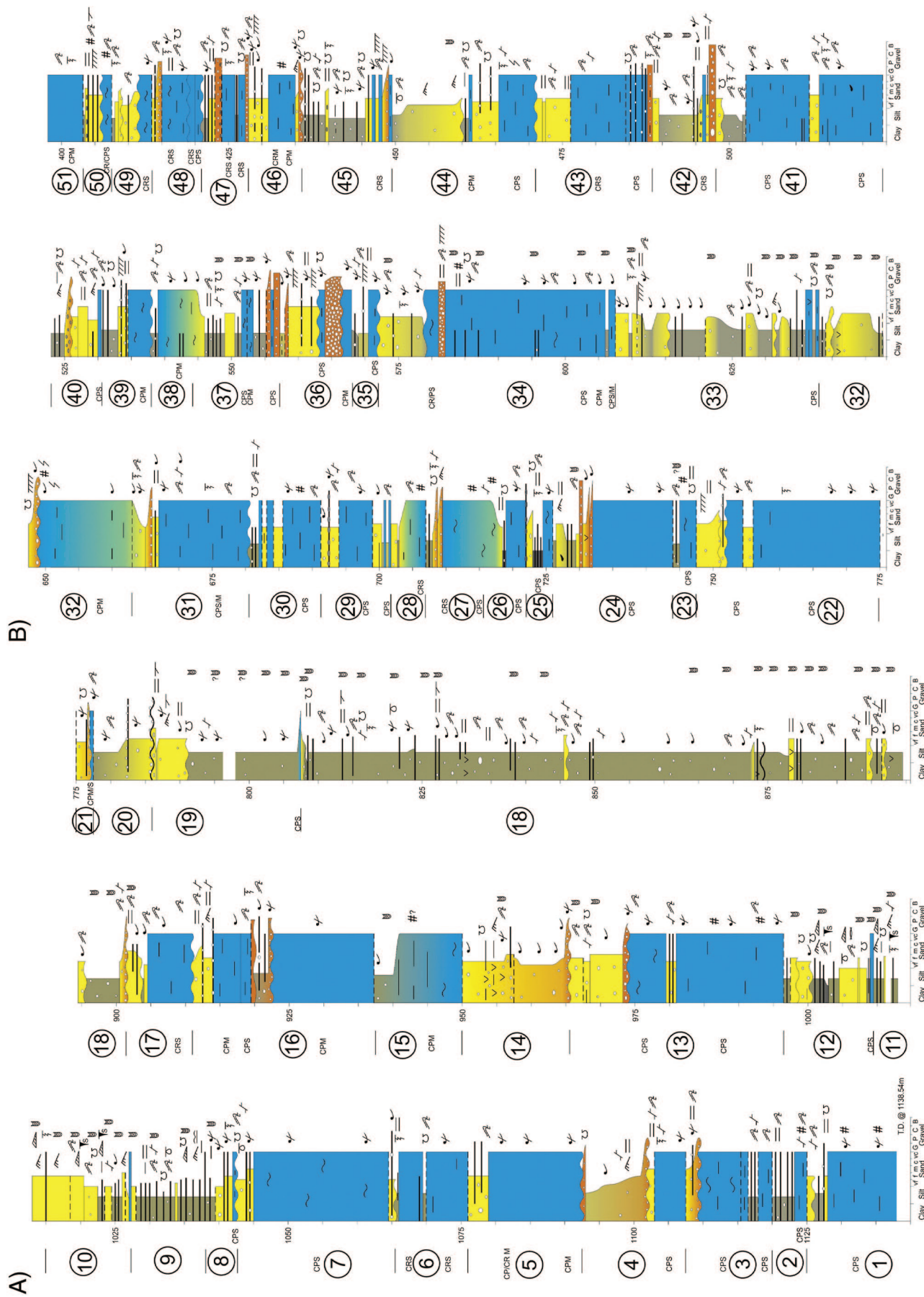
The succeeding coarsening-upward interval is interpreted as a Highstand Systems Tract (HST), formed when relative sea level peaked and began to drop during initiation of the next ice advance. The rate of sedimentation at this time began to exceed the rate of accommodation, and seabed transport by currents and waves facilitated the accumulation of fine-grained, texturally mature sands in deltas and other prograding, near-shore depositional systems. The sequence is capped at the contact with the overlying diamictite as advancing ice pushed proglacial debris basinward and initiated the next lowstand.

The AND-2A drillcore has been divided into a series of seventy-four sequences, from 0.92 to 93.89 m thick (Figure 3). Each sequence is defined on objective criteria. Specifically, each sequence contains both a coarse-grained lower interval that preserves evidence for ice-proximal conditions, and an overlying fine-grained division that contains evidence for ice-distal conditions (fine-grained Facies 1–3), not merely a parting within a coarse-grained facies unit (Figure 3). From the available geochronological data (Acton et al., 2008; SMS Science Team, 2010), it is likely that sequences were formed over timeframes coincident with the Milankovitch band, and can therefore be considered as high-frequency (fourth- or fifth-order of some workers: Vail et al., 1991; Catuneanu, 2006) sequences.

Each of the seventy-four sequences is bounded by a basinward shift in facies (sequence boundary), interpreted to record abrupt shallowing in paleobathymetry and in many cases (though not all), significant erosion (Figure 3). The top of most sequences in the AND-2A core is abrupt and erosional, although some show a continuously coarsening-upward trend into the overlying sequence (Figures 3 & 5). Some sequences show truncation of the upper coarsening-upward section, with diamictite of the succeeding sequence abruptly overlying mudrocks or muddy sandstones (Figure 3). Some such sequences, particularly in the uppermost 225 m of the core, are diamictite-dominated and may be composites of two or more sequences. On the other hand, some of the thicker sequences show development of multiple coarsening-upward or interbedded mudrock/sandstone intervals that can be interpreted as parasequences within the Highstand Systems Tract.

The fact that evidence for relative sea-level drawdown within each sequence coincides with evidence for increased proximity of glaciers suggests that geodynamic effects were minor relative to eustatic effects during the accumulation of this succession (in turn suggesting that any grounded ice across the drillsite was of only modest thickness). Furthermore, the fact that cyclicity is so clearly and persistently recorded in the Miocene stratigraphy suggests that the climatic regime remained dynamic through this interval (20.2–14.5 Ma).

The younger section (<14 Ma to present) is relatively condensed in stratigraphic thickness and overlies a major unconformity at 224.82 mbsf. The Upper Neogene section nonetheless reflects glacial cyclicity, in that fourteen sequences are preserved between 225 and 40 mbsf indicating that a dynamic ice sheet margin existed through this time. An expanded Upper Neogene section was recovered in the first ANDRILL core (AND-1B) and was found to preserve more than sixty genetic sequences similar to those described herein (Krissek et al., 2007; McKay et al., 2009; Naish et al., 2009), further supporting the interpretation of a dynamic glacial-marine environment through this time.



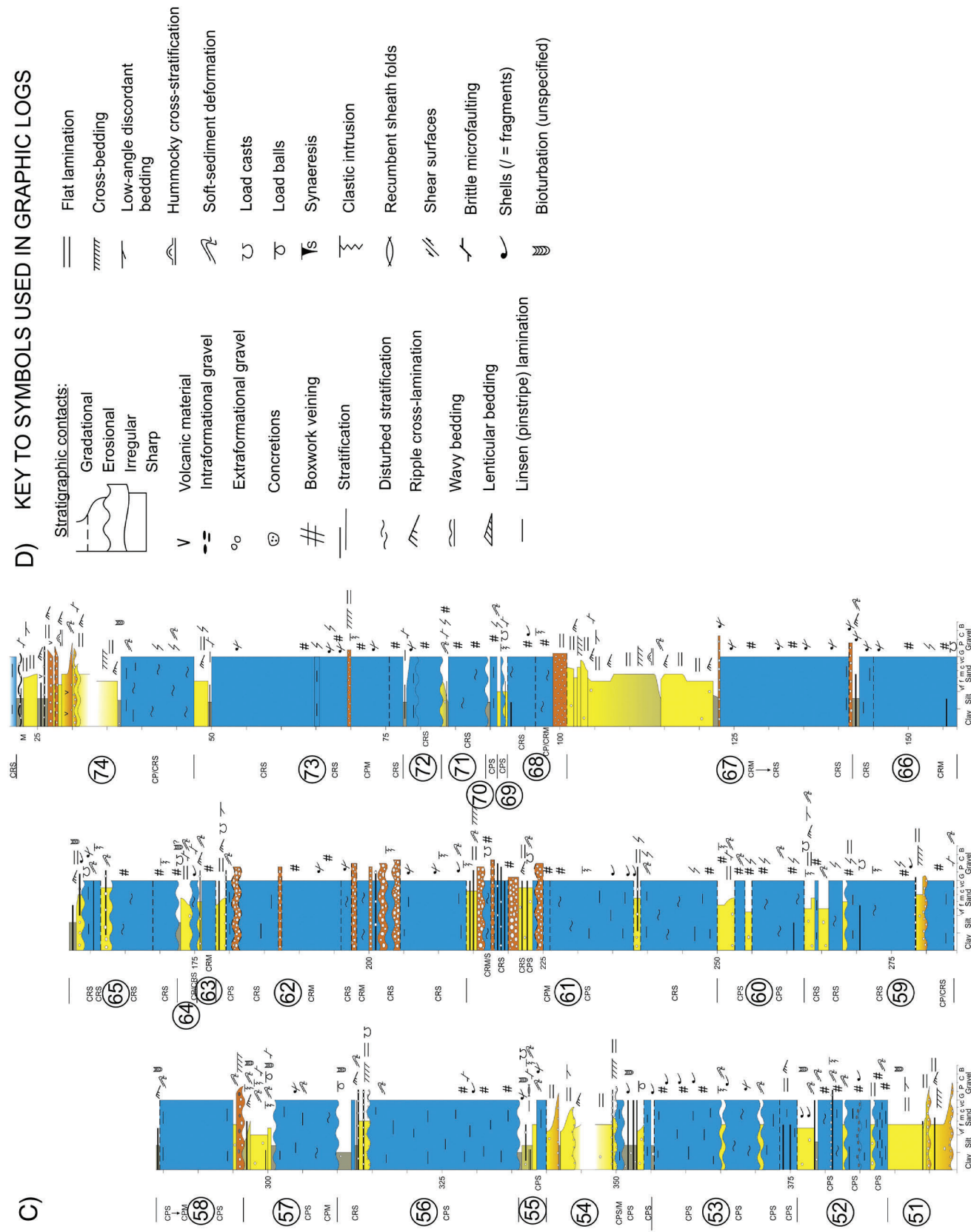


Figure 3. A–C) Detailed graphic log of the AND-2A core, showing the basis for subdivision of the succession into seventy-four sequences, and D) key to symbols used in graphic logs. Depth in meters below sea floor.

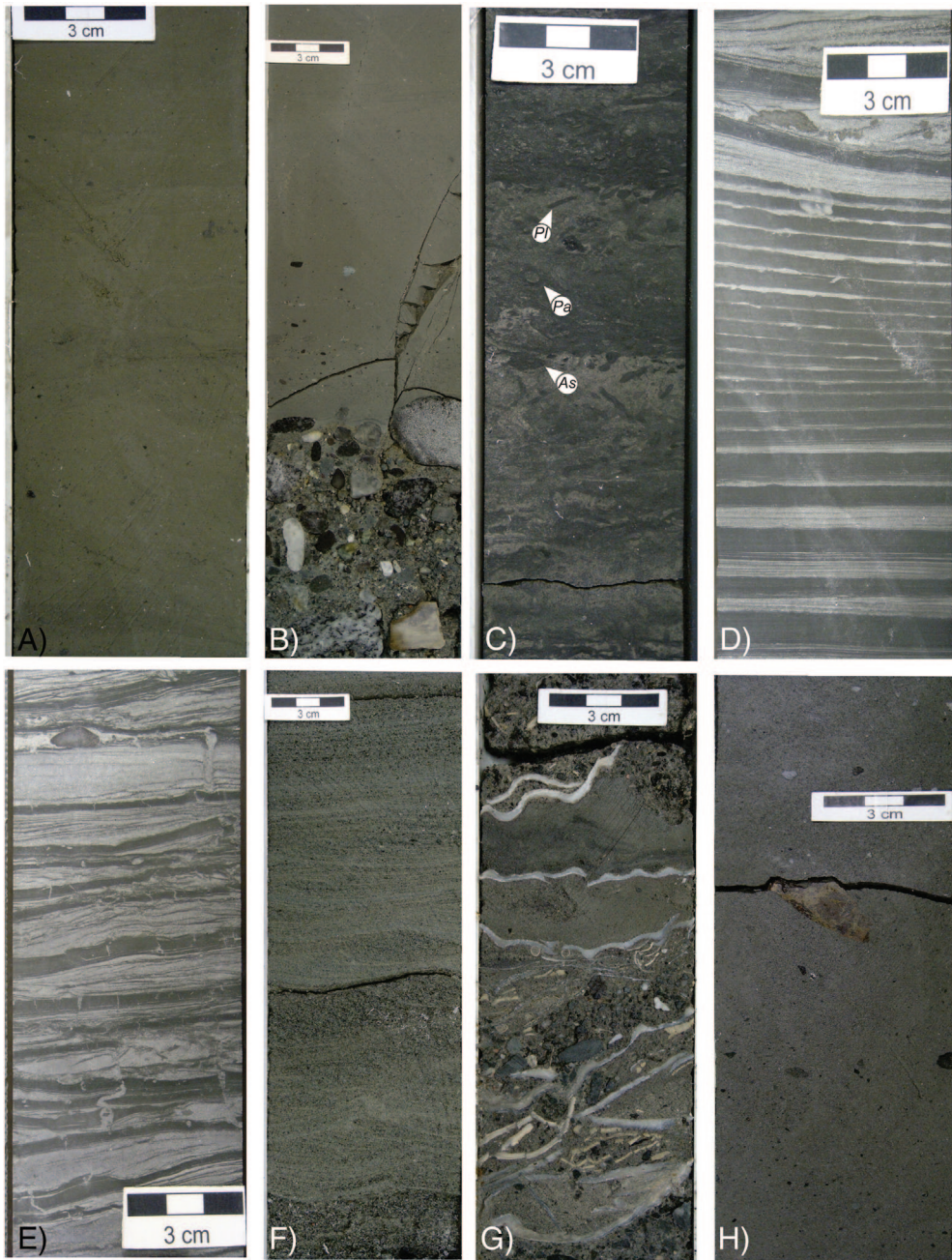
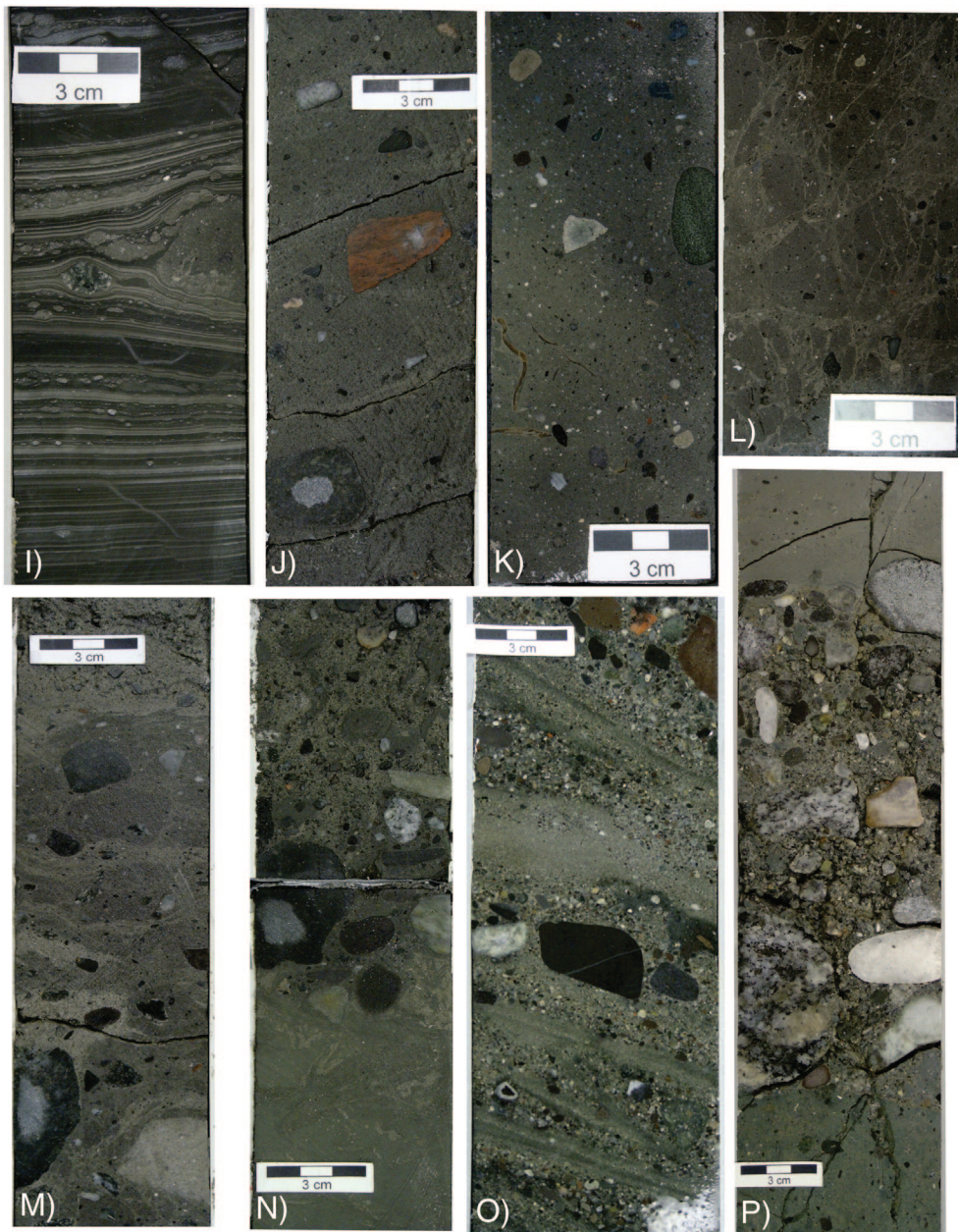


Figure 4. Core photographs of the various lithofacies recognized in AND-2A (Table 1). **A)** Facies 1 diatomite at 310.73–310.90 mbsf showing crude stratification and little to no dispersed gravel. **B)** Facies 1 mudrock abruptly overlying a Facies 9 conglomerate bed at 122.47–122.77 mbsf. The conglomerate, which overlies a thick diamictite (Sequence 67; Figure 3), is interpreted as a transgressive lag, and is overlain by mudstones representing the maximum flooding phase of the relative sea-level cycle. **C)** Facies 2 interbedded siltstone and fine-grained sandstone, partially homogenized by bioturbation (mainly *Planolites* (*Pl*), *Palaeophycus* (*Pa*) and *Asterosoma* (*As*)) at 1034.95–1035.11 mbsf. **D)** Facies 3 rhythmically interlaminated siltstone and fine-grained sandstone from 1029.91 to 1003.05 mbsf. **E)** Facies 3 rhythmically interbedded siltstone and fine-grained sandstone showing sparse bioturbation and abundant synaeresis cracks. **F)** Facies 4 ripple cross-laminated and flat laminated, fine- and medium-grained sandstone from 178.76 to 179.00 mbsf. **G)** Facies 4 sandstone at 430.52–430.70 mbsf showing abundant shells and fragments of marine bivalves and other invertebrates. **H)** Facies 5 muddy sandstone with dispersed gravel (< 1%) at 510.31–510.52 mbsf. **I)** Facies 6 rhythmically interlaminated claystone, siltstone and diamictite with dispersed gravel at 635.59–635.75 mbsf. **J)** Facies 7 stratified diamictite at 332.64–332.82 mbsf. **K)** Facies 8 massive and fossiliferous diamictite at 905.80–905.96 mbsf. **L)** Facies 8 massive diamictite showing pervasive boxwork fracturing at 649.51–649.62 mbsf. **M)** Facies 7/8 diamictite showing wispy fabric that is interpreted as a suite of shear-related structures indicating pervasive internal deformation of the material. **N)** Abrupt contact between bioturbated and soft-sediment-deformed, admixed siltstone and sandstone (Facies 2) below and Facies 9 conglomerate above. This horizon is interpreted as a sequence boundary and is the nominated base of Sequence 58 (Figure 3). **O)** Facies 9 interbedded pebble conglomerate and sandstone with cross-stratification at 214.42–214.63 mbsf. **P)** Interval from 122.60 to 122.93 mbsf, showing a diamictite (Facies 8) abruptly overlain by a pebble conglomerate (Facies 9) and in turn overlain by a mudstone with little to no dispersed gravel (Facies 2). The conglomerate is interpreted to record a transgressive lag formed during postglacial transgression, and the overlying mudstone to record the ensuing maximum flooding event. This interval forms part of Sequence 67 (Figure 3). Facies 10–13 are described and illustrated in detail by Del Carlo et al. (2009).



2. Vertical changes in sequence character

Changes in sequence character occur through the cored succession, and are utilized to inform interpretations of changing long-term environmental conditions (and, in the upper part of the section, changing tectonic conditions (Figure 2)). These include: 1) variation in sequence thickness from 0.92 to 93.89 m; 2) changes in the variety and range of facies included in sequences; 3) changes in the completeness of sequences, in terms of systems tracts; 4) changes in the proportion of the sequence occupied by diamictites; and 5) changes in the character of diamictites (stratified or massive, internally deformed or not, and fossiliferous or not). While sequence thickness is likely to be in part a function of available accommodation and therefore dependent on subsidence regime, the other listed variables can be used to interpret changes in environmental conditions over geologic time periods. In general, the spectrum of sequence character in the AND-2A core is considerably more diverse than in the somewhat younger section penetrated by the AND-1B core (Krissek et al., 2007; McKay et al., 2009; Naish et al., 2009).

2.1. Stratigraphic “motifs”

McKay et al. (2009) defined three stratigraphic “motifs” that account for discrete intervals of the AND-1B core. Here, we modify that concept to account for the greater range of sequence variability encountered in AND-2A (Table 2, Figure 6). The AND-1B core for the most part recovered strata younger than those recovered in AND-2A, and the stratigraphic motifs represent more glacially-dominated conditions than were represented in AND-2A. We find representatives of McKay et al.’s (2009) Motif 1 in the uppermost 300 m of the core (Figure 2), but no representatives of their Motif 2 (in which sequences are composed only of diamictite and overlying diatomite), presumably because of the different paleogeographic setting of AND-2A. We do, however, recognize a Motif intermediate in character between McKay et al.’s (2009) Motifs 1 and 3, which we assign here to Motif 2. Motif 3 is well-represented in the lower and middle parts of the AND-2A core (Figure 3), and we define two additional Motifs, 4 and 5, to account for the greater variety of facies and sequence stacking patterns in AND-2A. Motif 4 is further subdivided into 4a and 4b to

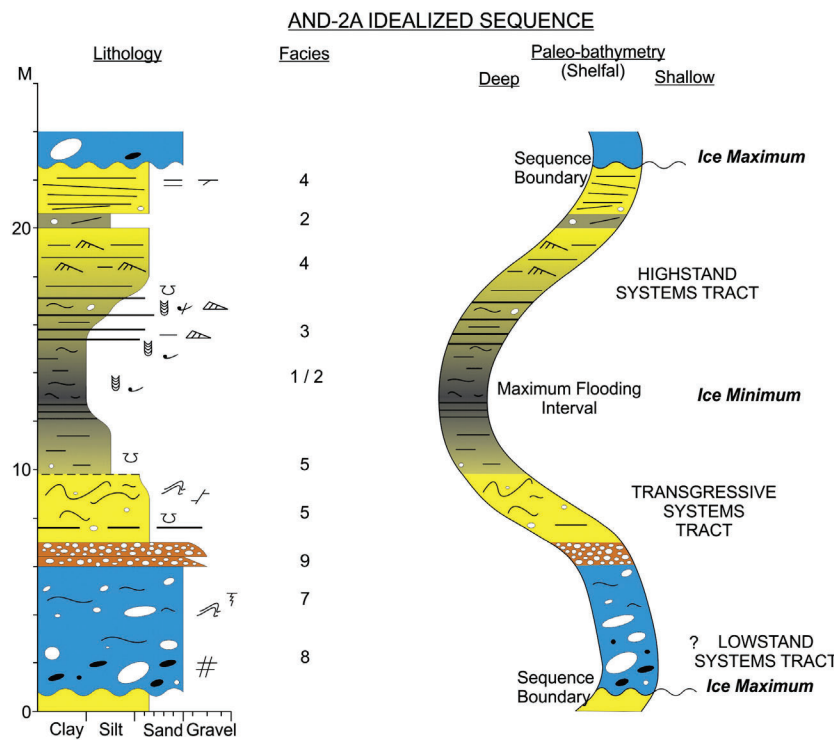


Figure 5. Diagram showing the facies stacking pattern and interpretation of an ideal, complete glacimarine sequence within the SMS core (based on Motif 3; Figure 7). See Figure 3D for key to symbols used. The basal sequence boundary is an abrupt contact overlain by a diamictite or other coarse-grained facies, which is interpreted to represent both a glacial maximum and a relative sea-level lowstand. This fines upward through muddy sandstones into mudrocks, recording the postglacial transgression and the Transgressive Systems Tract. Above a fine-grained, in many cases fossiliferous mudstone, which is interpreted as recording the Maximum Flooding Zone or Surface and a glacial minimum, a coarsening-upward succession of mudrocks into sandstones is interpreted to record the Highstand Systems Tract, and possibly in some cases a Forced Regressive Systems Tract heralding the onset of the next glacial advance. Variable proportions of this succession may have been removed by erosion associated with the following glacial advance and sea-level drawdown.

account for sandstone or mudrock-dominated sequences, respectively. Differences between motifs (Figure 6) are primarily in the diversity and relative abundance of different facies, reflecting varying environmental conditions. Cycle thickness was not considered a diagnostic characteristic, since this is influenced by a variety of external factors, in addition to environment.

Motif 1 (Figure 6A) is diamictite-dominated, with a relatively minor component of other lithologies, typically mainly mudrocks. Diamictites are typically unstratified, clast-rich, contain abundant intraformational clasts and sedimentary intrusions, and many preserve jigsaw-fit breccia fabrics and/or boxwork fracture/vein networks. Many diamictites in Motif 1 sequences also preserve rotational and other shear structures, and anomalously high bulk density/sonic velocity. The diamictites in Motif 1 sequences are interpreted to be ice-proximal, marine proglacial to subglacial deposits, formed under a dynamic climate regime that allowed repeated advance of glacial ice over the drillsite. Abundant evidence for grounded ice suggests that tidewater glaciers were grounded for consider-

able distances into the basin. This, together with the paucity of other facies, suggests a regime in which isostatic effects were significant, perhaps overwhelming eustatic sea-level fluctuations to produce a relatively subdued paleobathymetric curve (Figure 6A). A situation in which grounded ice frequently advanced across a slowly subsiding sea-floor explains the generally thin, incomplete and strongly top-truncated nature of Motif 1 sequences. A sub-polar glacial regime with minor meltwater influence is indicated by Motif 1, similar to that advocated for Motif 1 of McKay et al. (2009).

Motif 2 (Figure 6B) is also diamictite-dominated but involves a somewhat greater diversity and relative thickness of non-diamictite lithologies. Diamictites show a range of properties, but less abundant shear and breccia fabrics than their Motif 1 counterparts. Some are stratified, and many are soft-sediment-deformed. In addition to mudrocks, sandstones and conglomerates occur in Motif 2 sequences (e.g., Figure 6B). This is interpreted to reflect repeated tidewater glacial advances into the basin, with occasional grounded ice over the drillsite, producing a somewhat subdued

Table 2. Characteristics of stratigraphic motifs recognized within the AND-2A core.

Motif	Characteristics	Interpretation
1	Diamictite-dominated sequences, diamictites show shear and brecciation fabrics, are amalgamated, limited range and thickness of other lithologies	Cold, subpolar/polar glacial regime with minor meltwater involvement
2	Diamictite-dominated sequences, diamictites are more variable in character, are less amalgamated, greater range and abundance of other lithologies	Subpolar glacial regime with significant meltwater involvement
3	Sequences containing diverse lithologies including diamictites of varying character, sequences not diamictite-dominated	High-latitude temperate glacial regime, wet-based glaciers
4a	Sequences containing basal diamictites but dominated by stratified sandstones	High-latitude temperate glacial regime, distant wet-based glaciers
4b	Sequences containing basal diamictites but dominated by bioturbated and fossiliferous mudrocks	High-latitude temperate glacial regime, distant wet-based glaciers
5	Sequences containing thin basal diamictite or conglomerate but dominated by sandstones and mudrocks	Minimal (distal) glacial influence

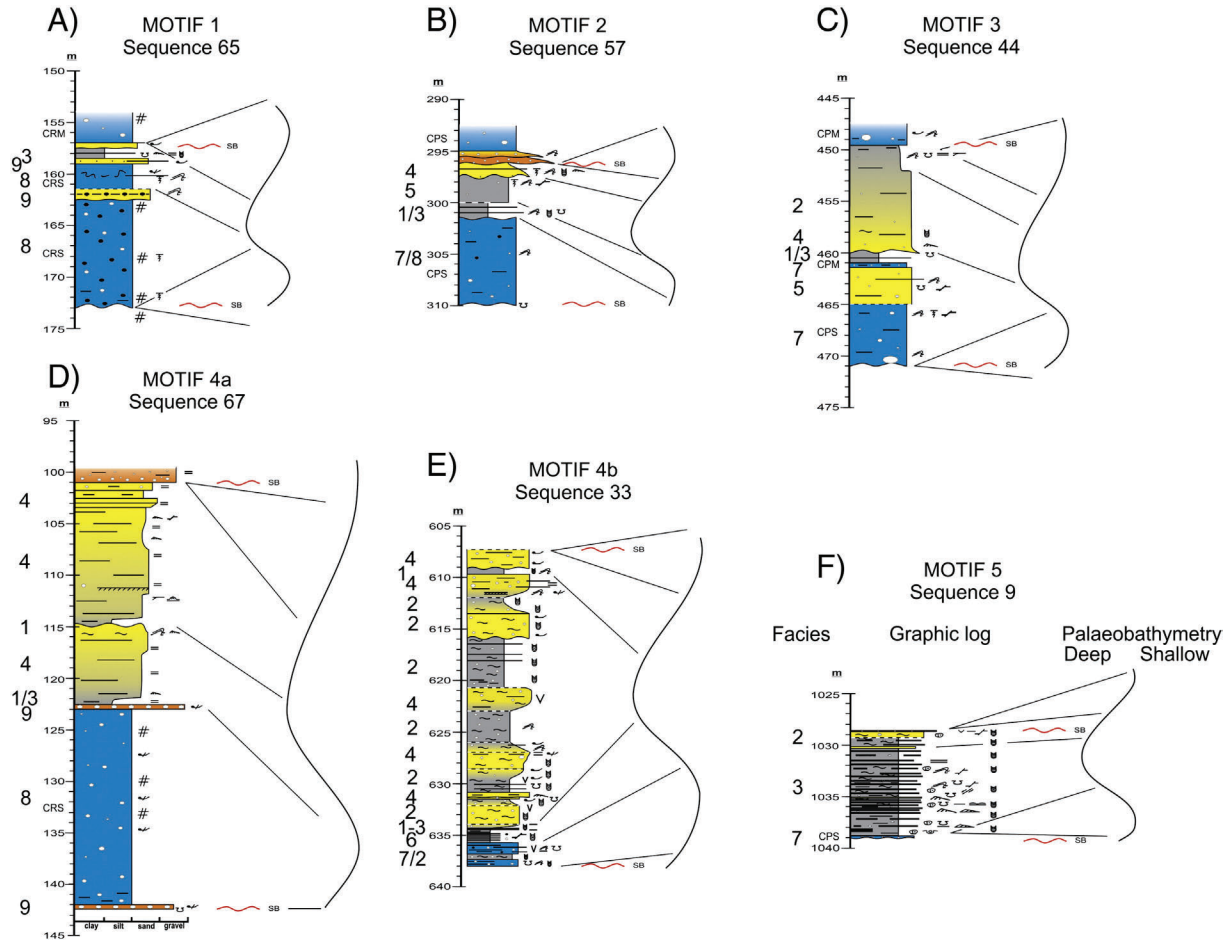


Figure 6. Graphic logs and interpreted paleobathymetry variation curve for each of the six Stratigraphic Motifs recognized within the AND-2A core. Motifs 1–5 are interpreted to record a spectrum of least to most ice-proximal and temperate to subpolar/polar climate. See Figure 3D for key to symbols used in graphic logs. Wavy red lines denote sequence boundaries. Motifs 1 and 3 were also recognized by McKay et al. (2009).

paleobathymetric variation curve. A sub-polar glacial regime with significant meltwater influence is indicated.

Motif 3 (Figure 6C) is lithologically diverse, typically containing a thinner diamictite than in Motifs 1 and 2, which is also in most cases stratified and does not contain shear structures or brecciation/boxwork veining. Mudrocks, representing maximum flooding, are represented, as are more abundant sandstones, both below and above the maximum flooding interval. Greater abundance of current- and wave-generated sedimentary structures, and of bioturbation, is characteristic of Motif 3. This is interpreted to record tidewater or floating tongue glaciers advancing periodically into the basin but not often across the drillsite, producing a more unmodified paleobathymetric variation curve (Figure 6C). A high-latitude, temperate glacial regime is suggested, with abundant meltwater influence (presumably from wet-based glaciers).

Motif 4 is also lithologically diverse, and involves significant thickness of either sandstones (Motif 4a; Figure 6D) or mudrocks (Motif 4b; Figure 6E). The only designated interval of Motif 4a is Sequence 67, enclosed between thick intervals of Motif 1 diamictite-dominated sequences. The preservation of a 20 m-thick succession of stratified sandstones is, however, considered inconsistent with Motif 1, and accordingly is defined as a separate motif (Figure 6D). Sandstones preserve abundant and well-preserved physical sedimentary structures, including flat and low-angle lamination, with local cross-bedding and probable hummocky cross-stratification, implying wave and current working of sand on a nearshore marine sediment surface, with minimal ice influence. Motif 4b is recognized in three separate intervals,

and comprises lithologically diverse sequences with typically thin, stratified diamictites overlain by mudrock-rich intervals and lesser sandstones (Figure 6E). Dispersed gravel is scattered throughout Motif 4b intervals, and bioturbation is both abundant and diverse. Motif 4 is interpreted to record times of glacial activity distal to the drillsite, allowing either sand deposition on an open marine shoreface (Motif 4a), or mud accumulation in more offshore marine shelf settings with intermittent supply of sand. A high-latitude, temperate glacial regime is implied with probably floating tongue glaciers that were distal to the drillsite except during glacial maxima.

Motif 5 (Figure 6F) describes thin, stratified or bioturbated diamictites overlain by thick intervals of mudrocks and sandstones. Dispersed gravel is relatively uncommon, while bioturbation is both diverse and widely distributed. Motif 5 is interpreted to record distal glacimarine deposition during periods of ice advance, and open marine conditions during glacial minima, giving rise to an unmodified curve of paleobathymetric variation (Figure 6E).

2.2. Vertical distribution of stratigraphic motifs

The seventy-four sequences are grouped into thirteen composite, lower-frequency sequences (equivalent to third-order sequences of Vail et al., 1991, Table 3), each defined by an internally consistent stratigraphic Motif (Figure 2). The stratigraphic motif may be considered as a proxy for climatic regime, allowing an interpretation of coherent, long-term climate variation over the period 20.2–14.5 Ma (Composite Sequences 1–10), and

Table 3. Details of composite (third-order) sequences in the AND-2A core. Age ranges are modified after SMS Science Team (2010).

Third-order sequence	Fourth/fifth-order sequences	Depth range	Age range	Motif	Characteristics	Major events
13	68–74	22.37–101.03 m	< 5.0 Ma > 750 ka	1	Diamictite-dominated, amalgamated	
12	67	101.03–142.34 m	?5.0–4.0 Ma	4a	Includes stratified shoreface sandstones	Pliocene warming
11	58–66	142.34–296.34 m	15.9–14.5 Ma and younger	1	Diamictite-dominated, amalgamated	
10	52–57	296.34–389.03 m	16.4–15.9 Ma	2	Diamictite-dominated, amalgamated	?Includes Mi2
9	46–51	389.03–436.18 m	16.5–16.4 Ma	3	Lithologically diverse including diamictites	
8	44–45	436.18–471.11 m	16.7–16.5 Ma	4b	Mudrocks, minor sandstones, few clasts	Warming event
7	34–43	471.11–607.35 m	17.3–16.7 Ma	3	Lithologically diverse including diamictites	
6	33	607.35–637.96 m	17.35–17.3 Ma	4b	Mudrocks, minor sandstones, few clasts	Warming event
5	22–32	637.96–774.94 m	17.8–17.35 Ma	2	Lithologically diverse including diamictites	?Mi1b
4	18–21	774.94–901.54 m	19.4–18.7 Ma	4b	Mudrocks, minor sandstones, few clasts	Ice-distal event
3	13–17	901.54–996.69 m	19.9–19.4 Ma	3	Lithologically diverse including diamictites	
2	8–12	996.69–1042.55 m	20.1–~20.05 Ma	5	Sandstones, heterolithic lithologies	Warming event
1	1–7	1042.55–1138.54 m	20.2–20.1 Ma	2	Lithologically diverse including diamictites	?Mi1a extension

a more fragmentary record for the period 14.5 to 0 Ma (Composite Sequences 11–13). The definition of these lower-frequency (higher-order) sequences will guide future discussion and provide a framework for correlation of events within and beyond the Antarctic continental margin. Given the age model (Acton et al., 2008; Di Vincenzo et al., 2010; SMS Science Team, 2010), it is possible to evaluate potential correlations between the AND-2A record and several major excursions identified in oxygen isotope records from the deep ocean basins for this interval of time (e.g., Miller et al., 1991, 1996). Composite Sequences 1 to 3 (~ 20.2–19.4 Ma) record an interval of mostly ice-proximal conditions in the middle Early Miocene (Figure 2). Within this section is an interval of ice-distal facies that denotes a time of probable warmth. Composite Sequence 2 (20.1 to ~ 20.05 Ma) is composed of five sequences all of which show thin basal diamictites and an abundance of ice-distal facies, collectively assigned to Motif 5 (Table 3; Figure 2 & 7). Composite Sequence 2 is unique within the SMS core in preserving coarsening-upward parasequences of probable deltaic and estuarine origin, and is quite unlike any Neogene facies assemblage yet recovered from the Antarctic continental margin. Composite Sequences 1 and 3 record major glacial events that are unrecognized in the deep-sea O¹⁸ records, or possibly represent temporal extensions of the Mi1a glaciation (21.8 Ma; Miller et al., 1996). The warm interval recorded by Composite Sequence 2 is not formally recognized by Miller et al. (1996), although one or more unnamed negative excursions in δ¹⁸O records may correspond to this interval.

The younger Composite Sequence 4 (19.4–18.7 Ma), is the thickest and most persistently fine-grained interval in the core (106 m-thick). It records a further period of relatively ice-distal conditions (Motif 4b; Table 3, Figure 2), though not as much so as Composite Sequence 2. Composite Sequence 5 (17.8–17.35 Ma) records an abrupt return to cold, ice-proximal conditions, and is characterized by thin sequences and limited lithological diversity. Given current geochronological constraints (Acton et al., 2008; Di Vincenzo et al., 2010; SMS Science Team, 2010), it is likely that this interval records the Mi1b glaciation at 17.7 Ma (Miller et al., 1996). Basement clasts from Composite Sequence 5 were found to reflect predominantly transport from the Skelton and Mulock glaciers to the south, and are interpreted by Sandroni and Talarico (2011) to record a major glaciation, potentially Mi1b.

Composite Sequence 6 (~ 17.35–17.3 Ma) comprises a single sequence that is more complete and lithologically diverse (Motif 4b; Table 3, Figure 2). This ice-distal interval is a little earlier than the onset of the Mid-Miocene Climatic Optimum (MMCO; cf. Holbourn et al., 2004, 2007) in proxy records. Composite Sequence 7 (17.3–16.7 Ma) preserves another transition into ice-proximal conditions. Composite Sequence 8 (16.7–16.5 Ma) preserves a further ice-distal succession (Motif 4b; Table 3, Figure 2), the uppermost such interval in the pre-14 Ma portion of the core. This Composite Sequence corresponds to a portion of the MMCO. Composite Sequences 6–10 collectively record base-

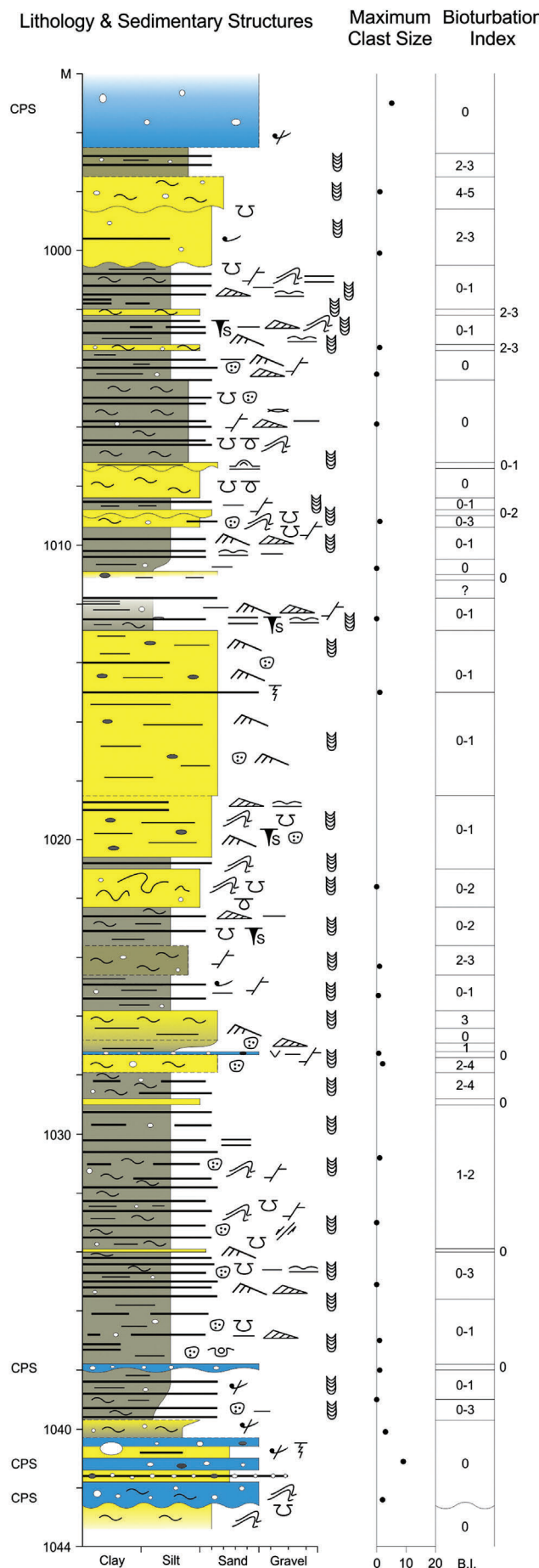
ment clasts derived from a variety of sources, including the nearby Koettlitz Glacier, a pattern interpreted by Sandroni and Talarico (2011) as recording fluctuating glaciers with periods of minimal ice extension into McMurdo Sound.

Above this, Composite Sequences 9–11 (16.5–14.5 Ma, and younger) illustrate a progressive trend towards further cooling of climate and more ice-proximal conditions, including the Mi2 glaciation at 16.3–16.1 Ma (Miller et al., 1996). However, this interval also contains a 2 m thick diatomaceous mudrock interval (312.11–310.04 mbsf) that shows evidence of ice-minimal conditions possibly coinciding with one of the stronger negative δ¹⁸O excursions noted by Holbourn et al. (2004, 2007). Evidence of more ice-proximal environments includes more extensive deformation and brecciation within diamictites indicating frequent grounding events. This interval may be interpreted as recording the aftermath of the MMCO and marks the onset of long-term cooling and expansion of the Antarctic ice sheets identified as the Mid-Miocene Transition in the deep-sea oxygen isotope record (e.g., Flower and Kennett, 1993; Shevenell et al., 2004; Holbourn et al., 2007). A major unconformity has been identified at 224.82 mbsf in the middle of Composite Sequence 11, separating Mid-Miocene strata below from a more fragmented younger succession above (Figure 2). The section above the unconformity is characterized by even less lithological diversity, a dominance of diamictites in sequences, and abundant deformation indicating frequent ice-grounding events. A further change into this interval is the upward disappearance of virtually all evidence of bioturbation. Composite Sequence 11 and part of 12 preserve basement clasts that include contributions from the Skelton and Mulock glaciers, interpreted by Sandroni and Talarico (2011) to represent a fragmented record of intense glacial conditions.

Composite Sequence 12 (?5.0–4.0 Ma) is similar to the section below but preserves in its upper part a substantial Transgressive/Highstand Systems Tracts interval of stratified, shoreface to inner shelf sandstones. The base of the stratified interval at 122.86 mbsf may coincide with a widely-correlated seismic stratigraphic event (Red reflector, Bclino of Fielding et al., 2008a) that is interpreted to record a Pliocene relative sea-level high at ~ 5.0–4.0 Ma. Composite Sequence 13 (< 5.0 Ma to > 750 ka), which contains inferred unconformities, represents an incomplete record of the Pliocene. It records the coldest climatic conditions in the entire core, comprising mainly massive diamictites with abundant internal deformation (Motif 1). The uppermost part of the interval preserves evidence of recent, basaltic volcanic activity proximal to the drillsite (Del Carlo et al., 2009; Di Vincenzo et al., 2010).

3. Stratigraphic significance of the AND-2A core

The AND-2A core represents an important new archive of Neogene paleoclimate evolution, preserving a relatively complete record of Early and early Middle Miocene time (Intervals 1–11), and a partial record of post-14.5 Ma (Intervals 12–13). The



younger AND-1B core was recovered from the flexural moat basin that surrounds Ross Island and provides a more complete record of the post-14.0 Ma interval (Naish et al., 2007, 2009). However, the latest Neogene record in the AND-2A core enhances results from earlier coring in the region, and further proves that sediment accumulated and has been preserved in locations proximal to East Antarctic glaciers post-14.0 Ma.

The most detailed paleoclimatic archive in the AND-2A core, however, is of the interval 20.2–14.5 Ma. Correlations can be made between the strata penetrated, the age model for the core (Acton et al., 2008; SMS Science Team, 2010), and published records of Antarctic paleoclimate evolution based primarily on oxygen isotope data from deep ocean drillcores. Records of the MMCO and the Mi1a, Mi1b and Mi2 glaciations (Miller et al., 1991, 1996) are likely preserved (Figure 2). But the AND-2A core, in addition to providing near-field ground-truth for these events, also identifies the character of other significant paleoclimatic changes that are not presently formally nominated in the literature. Foremost among these are the ice-minimum events recognized at 20.1–20.05 Ma (1040–997 mbsf; Figure 3 & 7) and 19.4–18.7 Ma (905–775 mbsf; Figure 3). Furthermore, the AND-2A core offers new information on the manner in which paleoenvironmental change was effected, and the long-term trends in paleoclimatic change. Cyclicity on the scale of 0.5–5 myr (third-order of Vail et al., 1991) is evident from the AND-2A core in addition to the shorter-term (fourth- and fifth-order) glacial-interglacial cyclicity manifested in the sequences shown in Figure 3 and Figure 6, which are likely in the Milankovitch band (cf. Holbourn et al., 2007). Efforts to extract eustatic sea-level trends from this interval of time have yielded only fragmentary records with minimal detail of individual excursions (Kominz et al., 2008, and see Figure 2). Records such as AND-2A have the potential to add significantly to this developing database. It is hoped that this new archive of Antarctic Neogene paleoenvironment will stimulate attempts to resolve further the complex Cenozoic history of Antarctica, and its ties into the global system.

4. Conclusions

The AND-2A core recovered from southern McMurdo Sound, Antarctica, shows a well-developed stratigraphic cyclicity. Seventy-four high-frequency (fourth- or fifth-order) glaciomarine sequences are recognized, and grouped into thirteen composite (third-order) sequences, each of which is internally characterized by a consistent stratigraphic stacking pattern, or Stratigraphic Motif. The distribution of the six stratigraphic motifs through the core informs an interpretation of Neogene paleoenvironmental change.

The basal portion of the core (1138–901 mbsf, composite Sequences 1–3: 20.2–19.4 Ma) shows evidence of austere, glacially-dominated conditions possibly representing an extension of the Mi1a glaciation of Miller et al. (1991), but punctuated by a period of distal ice conditions (Composite Sequence 2: 20.1–~20.05 Ma) that may correlate to a previously unrecognized negative isotope excursion (or major deglacial event). An overlying, mudrock-dominated stratal interval (901–775 mbsf, Composite Sequence 4: 19.4–18.7 Ma) records mainly ice-distal environments but with some evident glacial influence. A return to more ice-proximal environments is recorded in the interval 775–638 mbsf (Composite Sequence 5: 17.8–17.35 Ma), which possibly correlates to the Mi1b glaciation of Miller et al. (1991). The overlying Composite Sequence 6 (638–607 mbsf: 17.35–17.3 Ma) records a further period of ice retreat, which may be as-

Figure 7. Detailed graphic log of Composite Sequence 2, showing the ice-distal nature of sequences, and interpretation of intervals as deltaic and estuarine parasequences. See Figure 3D for key to symbols used. CPS – Clast-poor, sandy diamictites. Depth in meters below sea floor. Bioturbation Index (B.I.) after Bann et al. (2004), where B.I. = 0 represents absence of bioturbation and B.I. = 6 represents total destratification by bioturbation.

sociated with the onset of the Mid-Miocene Climatic Optimum (MMCO). Composite Sequence 7 (607–471 mbsf; 17.3–16.7 Ma) records a return to glacially proximal conditions. Composite Sequence 8 (471–436 mbsf; 16.7–16.5 Ma) marks a return to ice-distal conditions and may coincide with one of the warm periods of the MMCO. Composite Sequences 9–11 (16.5–14.5 Ma, and younger) record increasingly ice-proximal and climatically austere conditions, and include the Mi2 glaciation of Miller et al. (1991, 1996). These composite sequences highlight the variable nature of ice sheet behavior prior to and during the MMCO and indicate that the Antarctic margin remained glaciated through much of this inferred period of peak global warmth. Above a major unconformity at 225 mbsf, a truncated and partial record of post 14.5 Ma time is composed mainly of amalgamated, ice-proximal diamictite units, but includes a thick sandstone-dominated interval (part of Composite Sequence 12) that is believed to coincide with a regional Early Pliocene relative sea-level highstand at ~5.0–4.0 Ma.

The AND-2A core provides a hitherto unavailable, near-field record of dynamic paleoenvironmental history through the Early to Mid-Miocene. It allows new insights into climate change through this relatively poorly known interval of Earth history. In addition to providing direct sedimentary record of events recognized previously in proxy stable isotope records from the deep-sea (such as the onset of the MMCO), it also highlights some additional, previously unrecognized warm events in the Early Miocene. Future research might be able to utilize this spectacular record towards the finer-scale resolution of Neogene paleoclimate and paleoenvironmental change.

Acknowledgments

This paper is based on work supported by the National Science Foundation under Cooperative Agreement No. 0342484 through subawards administered by the ANDRILL Science Management Office (SMO) at University of Nebraska-Lincoln as part of the ANDRILL U.S. Science Support Program. We thank the SMS Drillsite and Science teams for their efforts in acquiring and characterizing the AND-2A core, and Steve Fischbein at the ANDRILL SMO for assistance with diagrams. The ANDRILL Program is a multinational collaboration between the Antarctic programs of Germany, Italy, New Zealand and the United States. Antarctica New Zealand is the project operator and developed the drilling system in collaboration with Alex Pyne at Victoria University of Wellington and Webster Drilling and Exploration Ltd. Antarctica New Zealand supported the drilling team at Scott Base; Raytheon Polar Services Corporation supported the science team at McMurdo Station and the Crary Science and Engineering Laboratory. The ANDRILL Science Management Office at the University of Nebraska-Lincoln provided science planning and operational support. Scientific studies are jointly supported by the US National Science Foundation (NSF), NZ Foundation for Research, Science and Technology (FRST), the Italian Antarctic Research Program (PNRA), the German Research Foundation (DFG) and the Alfred Wegener Institute for Polar and Marine Research (AWI). Editor David Bottjer and two anonymous referees are thanked for their reviews of the submitted manuscript.

References

- Abreu and Anderson, 1998** • V. S. Abreu and J. B. Anderson, Glacial eustasy during the Cenozoic: sequence stratigraphic implications, *American Association of Petroleum Geologists Bulletin* **82** (1998), pp. 1385–1400.
- Acton et al., 2008** • G. Acton, J. Crampton, G. Di Vincenzo, C. R. Fielding, F. Florindo, M. J. Hannah, D. M. Harwood, S. E. Ishman, K. Johnson, L. Jovane, R. H. Levy, B. Lum, M. C. Marcano, S. B. Mukasa, C. Ohneiser, M. Olney, C. Riesselman, L. Sagnotti, C. Stefano, E. Strada, M. Taviani, E. Tuzzi, K. L. Verosub, G. S. Wilson, and M. Zattin, Preliminary integrated chronostratigraphy of the AND-2A core, ANDRILL Southern McMurdo Sound Project Antarctica. In: D. M. Harwood, F. Florindo, F. Talarico, and R. H. Levy, Editors, *Studies from the ANDRILL, Southern McMurdo Sound Project, Antarctica, Terra Antarctica* **15** (2008), pp. 211–220.
- Andrews, 1974** • J. T. Andrews, Editor, *Glacial Isostasy*, Dowden, Hutchinson & Ross, Inc., Stroudsburg, PA (1974), 491 pp.
- Bamber et al., 2009** • J. L. Bamber, R. E. M. Riva, B. L. A. Vermeersen, and A. M. LeBrocq, Reassessment of the potential sea-level rise from a collapse of the West Antarctic Ice Sheet, *Science* **324** (2009), pp. 901–903.
- Bann et al., 2004** • K. L. Bann, C. R. Fielding, J. A. MacEachern, and S. C. Tye, Differentiation of estuarine and offshore marine deposits using integrated ichnology and sedimentology: Permian Pebbley Beach Formation, Sydney Basin, Australia. In: D. McIlroy, Editor, *The Application of Ichnology to Palaeoenvironmental and Stratigraphic Analysis*, Geological Society of London Special Publication **228** (2004), pp. 179–211.
- Barrett, 1986** • P. J. Barrett, Editor, *Antarctic Cenozoic history from the MS-STS-1 borehole, McMurdo Sound, New Zealand Department of Scientific and Industrial Research Bulletin* **237** (1986).
- Barrett, 1989** • P. J. Barrett, Editor, *Antarctic Cenozoic history from the CIROS-1 drillhole, McMurdo Sound, New Zealand Department of Scientific and Industrial Research Bulletin* **245** (1989).
- Barrett, 1996** • P. J. Barrett, Antarctic paleoenvironment through Cenozoic times – a review, *Terra Antartica* **3** (1996), pp. 103–119.
- Barrett, 2007** • P. J. Barrett, Cenozoic climate and sea level history from glacimarine strata off the Victoria Land coast, Cape Roberts Project, Antarctica. In: M. J. Hambrey, P. Christoffersen, N. F. Glasser and B. Hubbard, Editors, *Glacial Processes and Products*, International Association of Sedimentologists Special Publication **39** (2007), pp. 259–287.
- Barrett, 2009** • P. J. Barrett, A history of Antarctic Cenozoic glaciations – view from the margin. In: F. Florindo and M. Siegert, Editors, *Antarctic Climate Evolution, Developments in Earth and Environmental Sciences* **8**, Elsevier Science, Amsterdam (2009), pp. 33–83.
- Barrett and Hambrey, 1992** • P. J. Barrett and M. J. Hambrey, Plio-Pleistocene sedimentation in Ferrar Fiord, Antarctica, *Sedimentology* **39** (1992), pp. 109–123.
- Brotchie and Silvester, 1969** • J. F. Brotchie and R. Silvester, On crustal flexure, *Journal of Geophysical Research* **74** (1969), pp. 5240–5252.
- Catuneanu, 2006** • O. Catuneanu, Principles of Sequence Stratigraphy, Elsevier, Amsterdam (2006) 375 pp.
- Catuneanu et al., 2009** • O. Catuneanu, V. Abreu, J. Bhattacharya, M. D. Blum, R. W. Dalrymple, P. G. Eriksson, C. R. Fielding, W. L. Fisher, W. E. Galloway, M. R. Gibling, K. A. Giles, J. M. Holbrook, R. Jordan, C. G. Kendall, C. St. B. Macurda, O. J. Martinsen, A. D. Miall, J. E. Neal, D. Nummedal, L. Pomar, H. W. Posamentier, B. R. Pratt, J. F. Sarg, K. W. Shanley, R. J. Steel, A. Strasser, M. E. Tucker, and C. Winker, Towards the standardization of sequence stratigraphy, *Earth Science Reviews* **92** (2009), pp. 1–33.
- Cooper et al., 1987** • A. K. Cooper, F. J. Davey, and J. C. Behrendt, Seismic stratigraphy and structure of the Victoria Land Basin, western Ross Sea, Antarctica. In: A. K. Cooper and F. J. Davey, Editors, *The Antarctic continental margin: geology and geophysics of the western Ross Sea, Circum-Pacific Council for Energy and Mineral Resources, Earth Science Series* **5B** (1987), pp. 27–65 Houston, Texas.
- Del Carlo et al., 2009** • P. Del Carlo, K. S. Panter, K. Bassett, G. Di Vincenzo, and S. Rocchi, The upper lithostratigraphic unit of ANDRILL AND-2A core (Southern McMurdo Sound, Antarctica): local Pleistocene volcanic sources, paleoenvironmental implications and subsidence in the southern Victoria Land Basin, *Global and Planetary Change* **69** (2009), pp. 142–161.
- Di Vincenzo et al., 2010** • G. Di Vincenzo, L. Bracciali, P. Del Carlo, K. Panter, and S. Rocchi, ^{40}Ar – ^{39}Ar dating of volcanogenic products from the AND-2A core (ANDRILL Southern McMurdo Sound Project, Antarctica): correlations with the Erebus Volcanic Province and implications for the age model of the core, *Bulletin of Volcanology* **72** (2010), pp. 487–505.
- Dunbar and Barrett, 2005** • G. D. Dunbar and P. J. Barrett, Estimating paleobathymetry of wave-graded continental shelves from sediment texture, *Sedimentology* **52** (2005), pp. 253–269.
- Dunbar et al., 2008** • G. D. Dunbar, T. R. Naish, P. J. Barrett, C. R. Fielding, and R. D. Powell, Constraining the amplitude of Late Oligocene bathymetric changes in western Ross Sea during orbitally-induced oscillations in the East Antarctic Ice Sheet: 1. Implications for glacimarine sequence stratigraphic models, *Paleogeography, Paleoclimatology Palaeoecology* **260** (2008), pp. 50–65.
- Fielding and al., in press** • C. R. Fielding, D. M. Harwood, D. M. Winter, and J. E. Francis, Neogene stratigraphy of Taylor Valley, Transantarctic Mountains, Antarctica: evidence for climate dynamism and a vegetated early Pliocene coastline of McMurdo Sound. *Global and Planetary Change* (in press); doi:10.1016/j.gloplacha.2010.09.03.
- Fielding et al., 1998** • C. R. Fielding, K. J. Woolfe, J. A. Howe, and M. Lavelle, Sequence stratigraphic analysis of CRP-1, Cape Roberts Project, McMurdo Sound, Antarctica, *Terra Antartica* **5** (1998), pp. 353–361.
- Fielding et al., 2000** • C. R. Fielding, T. R. Naish, K. J. Woolfe, and M. A. Lavelle, Facies analysis and sequence stratigraphy of CRP-2/2A, McMurdo Sound, Antarctica, *Terra Antartica* **7** (2000), pp. 323–338.

- Fielding et al., 2006** • C. R. Fielding, S. A. Henrys, and T. J. Wilson, Rift history of the western Victoria Land Basin: a new perspective based on integration of cores with seismic reflection data. In: D. K. Futterer, D. Damaske, G. Kleinschmidt, H. Miller, and F. Tessenoohn, Editors, *Antarctica: Contributions to Global Earth Sciences*, Springer-Verlag, Berlin (2006), pp. 309–318.
- Fielding et al., 2008a** • C. R. Fielding, J. Whittaker, S. A. Henrys, T. J. Wilson, and T. R. Naish, Seismic facies and stratigraphy of the Cenozoic succession in McMurdo Sound, Antarctica: implications for tectonic, climatic and glacial history, *Palaeogeography, Palaeoclimatology, Palaeoecology* **260** (2008), pp. 8–29.
- Fielding et al., 2008b** • C. R. Fielding, C. B. Atkins, K. N. Bassett, G. H. Browne, G. B. Dunbar, B. D. Field, T. D. Frank, L. A. Krissek, K. S. Panter, S. Passchier, S. F. Pekar, S. Sandroni, F. Talarico, and ANDRILL-SMS Science Team, Sedimentology and stratigraphy of the AND-2A Core, ANDRILL Southern McMurdo Sound Project, Antarctica. In: D. M. Harwood, F. Florindo, F. Talarico, and R. H. Levy, Editors, *Studies from the ANDRILL Southern McMurdo Sound Project, Antarctica*, *Terra Antarctica* **15** (2008), pp. 77–112.
- Flower and Kennett, 1993** • B. P. Flower and J. P. Kennett, Middle Miocene ocean-climate transition; high-resolution oxygen and carbon isotopic records from Deep Sea Drilling Project Site 588A, southwest Pacific, *Paleoceanography* **8** (1993), pp. 811–843.
- Flower and Kennett, 1994** • B. P. Flower and J. P. Kennett, The middle Miocene climatic transition: East Antarctic ice sheet development, deep ocean circulation and global carbon cycling, *Palaeogeography, Palaeoclimatology, Palaeoecology* **108** (1994), pp. 537–555.
- Harwood et al., 2008** • D. M. Harwood, F. Florindo, F. Talarico, and R. Levy, Editors, *Studies from the ANDRILL Southern McMurdo Sound Project, Antarctica*, *Terra Antarctica* **15** (2008), pp. 1–235.
- Henrys et al., 2007** • S. A. Henrys, T. J. Wilson, J. M. Whittaker, C. R. Fielding, J. Hall, and T. R. Naish, Tectonic history of mid-Miocene to present southern Victoria Land Basin, inferred from seismic stratigraphy in McMurdo Sound, Antarctica, *USGS Open-File Report-2007-1047, Short Research Paper 049*, National Academies Press (2007); doi: 10.3133/of2007-1047.srp049.
- Holbourn et al., 2004** • A. Holbourn, W. Kuhnt, J. A. Simo, and Q. Y. Li, Middle Miocene isotope stratigraphy and paleoceanographic evolution of the northwest and southwest Australian margins (Wombat Plateau and Great Australian Bight), *Palaeogeography, Palaeoclimatology, Palaeoecology* **208** (2004), pp. 1–22.
- Holbourn et al., 2007** • A. Holbourn, W. Kuhnt, M. Schulz, J.-A. Flores, and N. Andersen, Orbitally-paced climate evolution during the Middle Miocene “Monterey” carbon-isotope excursion, *Earth and Planetary Science Letters* **261** (2007), pp. 534–550.
- Kominz et al., 2008** • M. A. Kominz, J. V. Browning, K. G. Miller, P. J. Sugerman, S. Mizintseva, and C. R. Scotese, Late Cretaceous to Miocene sea-level estimates from the New Jersey and Delaware coastal plain coreholes: An error analysis, *Basin Research* **20** (2008), pp. 211–226.
- Krissek et al., 2007** • L. Krissek, G. Browne, L. Carter, E. Cowan, G. Dunbar, R. McKay, T. Naish, R. Powell, J. Reed, T. Wilch, and ANDRILL-MIS Science Team, Sedimentology and stratigraphy of AND-1B core, ANDRILL McMurdo Ice Shelf Project, Antarctica, *Terra Antarctica* **14** (2007), pp. 185–222.
- Lear et al., 2004** • C. H. Lear, Y. Rosenthal, H. K. Coxall, and P. A. Wilson, Late Eocene to early Miocene ice sheet dynamics and the global carbon cycle, *Paleoceanography* **PA4015** (2004), pp. 1–11.
- Lewis et al., 2008** • A. R. Lewis, D. R. Marchant, A. C. Ashworth, L. Hedenaes, S. R. Hemming, J. V. Johnson, M. J. Leng, M. L. Machlus, A. E. Newton, J. I. Raine, J. K. Willenbring, M. Williams, and A. P. Wolfe, Mid-Miocene cooling and the extinction of tundra in continental Antarctica, *Proceedings of the National Academy of Sciences* **105** (2008), pp. 10676–10680.
- Lønne, 2001** • I. Lønne, Dynamics of marine glacier termini read from moraine architecture, *Geology* **29** (2001), pp. 199–202.
- Lønne and Syvitski, 1997** • I. Lønne and J. P. Syvitski, Effects of the readvance of an ice margin on the seismic character of the underlying sediment, *Marine Geology* **143** (1997), pp. 81–102.
- McGinnis, 1981** • L. D. McGinnis, Editor, *Dry Valley Drilling Project, American Geophysical Union Antarctic Research Series* **33** (1981) Washington, D. C., 465 pp.
- McKay et al., 2009** • R. McKay, G. Browne, L. Carter, E. Cowan, G. Dunbar, L. Krissek, T. Naish, R. Powell, J. Reed, F. Talarico, and T. Wilch, The stratigraphic signature of the late Cenozoic Antarctic Ice Sheets in the Ross Embayment, *Geological Society of America Bulletin* **121** (2009), pp. 1537–1561.
- Miller et al., 1991** • K. G. Miller, J. D. Wright, and R. G. Fairbanks, Unlocking the ice house: Oligocene–Miocene oxygen isotopes, eustasy and margin erosion, *Journal of Geophysical Research* **96** (1991), pp. 6829–6848.
- Miller et al., 1996** • K. G. Miller, G. S. Mountain, Leg 150 Shipboard Party, and Members of the New Jersey Coastal Plain Drilling Project, Drilling and dating New Jersey Oligocene–Miocene sequences: Ice volume, global sea level, and EXXON records, *Science* **271** (1996), pp. 1092–1095.
- Mitrovica and Vermeersen, 2002** • J. X. Mitrovica and L. L. A. Vermeersen, Glacial isostatic adjustment and the Earth system. In: J. X. Mitrovica and L. L. A. Vermeersen, Editors, *Ice Sheets, Sea Level and the Dynamic Earth, Washington, D. C.*, American Geophysical Union Geodynamics Series **29** (2002), pp. 1–2.
- Mitrovica et al., 2009** • J. X. Mitrovica, N. Gomez, and P. U. Clark, The sea-level fingerprint of West Antarctic collapse, *Science* **323** (2009), p. 753.
- Naish et al., 2007** • T. R. Naish, R. D. Powell and R. Levy, Editors, *Studies from the ANDRILL McMurdo Ice Shelf Project, Antarctica, Terra Antarctica* **14** (2007), pp. 110–328.
- Naish et al., 2008** • T. R. Naish, G. S. Wilson, G. B. Dunbar, and P. J. Barrett, Constraining the amplitude of Late Oligocene bathymetric changes in western Ross Sea during orbitally-induced oscillations in the East Antarctic Ice Sheet: (2) Implications for global sea-level changes, *Palaeogeography, Palaeoclimatology, Palaeoecology* **260** (2008), pp. 66–76.
- Naish et al., 2009** • T. Naish et al., Late Cenozoic stability of the West Antarctic Ice Sheet, *Nature* **458** (2009), pp. 322–329; doi:10.1038/nature07867.
- Passchier et al., in press** • S. Passchier, G. Browne, B. Field, C. R. Fielding, L. A. Krissek, K. Panter, S. F. Pekar, and ANDRILL-SMS Science Team, Early and Middle Miocene Antarctic glacial history from the sedimentary facies distribution in AND-2A, Ross Sea, Antarctica, *Geological Society of America Bulletin* (in press). doi: 10.1130/B30334.1
- Sandroni and Talarico, 2011** • S. Sandroni and F. Talarico, The record of Miocene climatic events in AND-2A drill core (Antarctica): Insights from provenance analyses of basement clasts, *Global and Planetary Change* **75** (2011), pp. 31–46.
- Shevenell et al., 2004** • A. E. Shevenell, J. P. Kennett, and D. Lea, Middle Miocene Southern Ocean cooling and Antarctic cryosphere expansion, *Science* **305** (2004), pp. 1766–1770.
- SMS Science Team, 2010** • SMS Science Team, An integrated age model for the ANDRILL-2A drill core. In: K. Kontar, D. M. Harwood, F. Florindo, and S. Fischbein, compilers, ANDRILL Southern McMurdo Sound Project Science Integration Workshop, Erice, Italy, 6–11th April, 2010, ANDRILL Contribution 16, 12–13.
- Sugden et al., 1993** • D. E. Sugden, D. R. Marchant, and G. H. Denton, The case for a stable East Antarctic Ice Sheet, *Geografiska Annaler* **75** (1993), pp. 151–353.
- Taviani et al., 2008** • M. Taviani, M. Hannah, D. M. Harwood, S. E. Ishman, K. Johnson, M. Olney, C. Riesselman, E. Tuzzi, R. Askin, A. G. Beu, S. Blair, V. Cantarelli, A. Ceregato, S. Corrado, B. Mohr, S. H. H. Nielsen, D. Persico, S. Petrushak, J. I. Raine, S. Warny, and ANDRILL-SMS Science Team, Palaeontological characterization and analysis of the AND-2A core, ANDRILL Southern McMurdo Sound Project, Antarctica, *Terra Antarctica* **15** (2008), pp. 113–146. V
- Vail et al., 1991** • P. R. Vail, F. Audemard, S. A. Bowman, P. N. Eisner, and C. Perez-Cruz, The stratigraphic signatures of tectonics, eustasy and sedimentology – An overview. In: G. Einsele, W. Ricken, and A. Seilacher, Editors, *Cycles and Events in Stratigraphy*, Springer-Verlag, Berlin (1991), pp. 617–659.
- Vincent and Berger, 1985** • E. Vincent and W. H. Berger, Carbon dioxide and polar cooling in the Miocene: the Monterey hypothesis. In: E. T. Sundquist and W. S. Broecker, Editors, *The carbon cycle and atmospheric CO₂: natural variations Archean to present*, *Geophysical Monograph* **32**, AGU, Washington, D. C. (1985), pp. 455–468.
- Webb et al., 1984** • P. -N. Webb, D. M. Harwood, B. C. McKelvey, J. H. Mercer, and L. D. Stott, Cenozoic marine sedimentation and ice volume variation in the East Antarctic craton, *Geology* **12** (1984), pp. 287–291.
- Woodruff and Savin, 1991** • F. Woodruff and S. Savin, Mid-Miocene isotope stratigraphy in the deep sea: high-resolution correlations, paleoclimatic cycles, and sediment preservation, *Paleoceanography* **6** (1991), pp. 755–806.
- Zachos et al., 2001** • J. Zachos, M. Pagani, L. Sloan, E. Thomas, and K. Billups, Trends, rhythms, and aberrations in global climate 65 Ma to present, *Science* **292** (2001), pp. 686–693.